Endothelial Cell Migration and Vascular Endothelial Growth Factor Expression Are the Result of Loss of Breast Tissue Polarity

Amy Chen,[1] Ileana Cuevas,[1] Paraic A. Kenny,[2,3] Hiroshi Miyake,[1] Kimberley Mace,[1] Cyrus Ghajar,[2] Aaron Boudreau,[2] Mina Bissell,[2] and Nancy Boudreau[1]

[1]Surgical Research Laboratory, Department of Surgery, University of California at San Francisco, San Francisco, California; [2]Life Sciences Division, Lawrence Berkeley National Laboratory, Berkeley, California; and [3]Department of Developmental and Molecular Biology, and Albert Einstein Cancer Center, Albert Einstein College of Medicine, Bronx, New York

Abstract

Recruiting a new blood supply is a rate-limiting step in tumor progression. In a three-dimensional model of breast carcinogenesis, disorganized, proliferative transformed breast epithelial cells express significantly higher expression of angiogenic genes compared with their polarized, growth-arrested nonmalignant counterparts. Elevated vascular endothelial growth factor (VEGF) secretion by malignant cells enhanced recruitment of endothelial cells (EC) in heterotypic cocultures. Significantly, phenotypic reversion of malignant cells via reexpression of HoxD10, which is lost in malignant progression, significantly attenuated VEGF expression in a hypoxia-inducible factor 1α–independent fashion and reduced EC migration. This was due primarily to restoring polarity: forced proliferation of polarized, nonmalignant cells did not induce VEGF expression and EC recruitment, whereas disrupting the architecture of growth-arrested, reverted cells did. These data show that disrupting cytostructure activates the angiogenic switch even in the absence of proliferation and/or hypoxia and restoring organization of malignant clusters reduces VEGF expression and EC activation to levels found in quiescent nonmalignant epithelium. These data confirm the importance of tissue architecture and polarity in malignant progression. [Cancer Res 2009;69(16):6721–9]

Introduction

It is well established that solid tumors require angiogenesis to survive (1, 2) and changes in the breast tumor microenvironment promote formation of new blood vessels (3–5) with high angiogenic potential linked to poor prognosis (4, 6).

In breast tumors, several key angiogenic factors have been identified, the most prominent being vascular endothelial growth factor (VEGF), which acts on adjacent endothelial cells (EC) through the VEGF receptor 2, initiating growth, migration, and invasion into adjacent tumor stroma. Recent clinical studies have shown that function-blocking antibodies against VEGF significantly impair tumor progression (7).

In the earliest stages of malignant breast cancer [i.e., ductal carcinoma *in situ* (DCIS)], VEGF may be induced by the increased metabolic demand and hypoxia (8), as low oxygen tension stabilizes hypoxia-inducible factor 1α (HIF1α), which binds to, and activates, transcription of the VEGF promoter (see ref. 9 for review). Yet, paradoxically, most cells suspend mRNA translation and protein synthesis when faced with either nutrient depletion or hypoxia (10, 11) and suggests that additional changes in the breast tumor microenvironment may facilitate expression of angiogenic factors.

Sustained signaling through α6β4 integrin and elevated phosphatidylinositol 3-kinase (PI3K) levels also enhance translation of VEGF mRNA in carcinoma cells (12), and even in the absence of hypoxia, both PI3K and mitogen-activated protein kinase (MAPK) signaling are elevated in breast tumors and can increase the transcription and secretion of VEGF independent of HIF1α (13, 14). Expression of the transcription factor HoxB7 also increases VEGF expression in both breast and other epithelial tumor cells; similarly, β-catenin activation can induce the expression of angiogenic factors, including VEGF (15, 16). Thus, a variety of changes in breast tumor cells conspire to activate expression of angiogenic factors.

Identifying features of the normal breast microenvironment, which collectively normalize MAPK and PI3K, sequester β-catenin, and/or attenuate α6β4 expression, may prove to be key in inhibiting the angiogenic switch. Several studies by our group have shown that breast tissue architecture plays a fundamental role in mediating each of these pathways (17–20). Further, despite many genetic defects, malignant breast epithelial cells, which exhibit a proliferative, unpolarized morphology when grown in three-dimensional cultures (21), can be reverted to a polarized, acinar morphology and growth arrested by agents targeting the MAPK and PI3K pathways (17–19, 22). We have also shown that restoring expression of a key morphoregulatory gene, *HoxD10*, lost in tumorigenic breast epithelial cells reverts tumorigenic breast cells to a growth-arrested and organized phenotype (23). Whether the paralogous *HoxA10* gene, which is also lacking in some breast tumors (24), also stabilizes breast tissue architecture is not known. Nonetheless, considering the remarkable dominance of the reverted tumor cell phenotype over the tumor cell genotype, we hypothesized that proper organization of breast epithelial cells may suppress expression of angiogenic factors, thus implicating loss of tissue organization as a key activator of the angiogenic switch in breast cancer.

Materials and Methods

Cell culture. Immortalized human dermal microvascular EC HMEC-1 [a gift from T. Lawley (25), Emory University, Atlanta, GA], the human breast epithelial cell line MDA-MB-231 (American Type Culture Collection), and epithelial cell lines HMT-3522 T4-2, S-1, and S1 epidermal growth factor receptor (EGFR) were grown and maintained in two- and three-dimensional cultures as previously described (18, 19).

Note: M. Bissell and N. Boudreau contributed equally to this work.

Requests for reprints: Nancy Boudreau, Surgical Research Laboratory, Department of Surgery, University of California at San Francisco, Box 1302, San Francisco, CA 94143. Phone: 415-206-6951; Fax: 415-206-6997; E-mail: nancyjb@itsa.ucsf.edu.

doi:10.1158/0008-5472.CAN-08-4069

Epithelial/endothelial cocultures and migration assay. Cell migration assays were performed using a modification of procedures previously described (23, 26). Briefly, 6.5-mm Transwell chambers (8-μm pore; Corning) were coated with 10 μg/mL of type I collagen (Cohesion Tech), and 5×10^4 serum-starved HMEC-1 cells were plated in 300 μL of fibroblast basal medium (FBM; Lonza) containing 0.5% bovine serum albumin (BSA).

For coculture experiments, T4-2, S1, or MDA-MB-231 cells were cultured using polymerized laminin-rich extracellular matrix (lrECM; Matrigel, BD Biosciences) for 72 and 16 h before assays, the medium was changed to serum-free FBM, and Transwell inserts with EC were added to the upper chamber. After 4 h at 37°C, ECs on the upper surface were removed and HMEC-1 cells that migrated onto the bottom of the membrane were stained with Diff-Quick (VWR Scientific Products) and five fields in each well were counted by phase-contrast microscopy (magnification, ×20). When indicated, HMEC-1 cells were preincubated for 30 min with 0.5 μg/mL of control IgG or a monoclonal antibody against anti-human VEGF (R&D Systems).

Retroviral vectors and transduction. The human 1,100-bp HoxD10 cDNA (Genbank accession no. X59373) was cloned into the *Eco*RI site of the pBABE retroviral vector (Clontech). T4-2 and T4-2 Rac1L61 cells were transduced with control plasmid (pBABE) or pBD10 and selected in 0.5 μg/mL puromycin (Sigma) as previously described (23).

Reverse transcription/PCR. Cells grown in three-dimensional cultures were released from lrECM using previously described procedures (18, 23), and cell pellets were resuspended in RNA lysis buffer and extracted using the RNeasy Mini isolation kit (Qiagen). One microgram of total RNA was reverse transcribed using Moloney murine leukemia virus reverse transcriptase (Qiagen), and one twenty-fifth of this reaction was linearly amplified for 30 cycles (VEGF and HoxD10) of denaturation (30 s at 95°C), annealing (30 s at 51°C for VEGF; 58°C for HoxD10), and extension (30 s at 72°C) in a thermal cycler (PTC-200 Peltier thermal cycler, M.J. Research). The following primers were used: HoxD10, 5′-CTGTCATGCTCCAGCTCAACCC-3′ (forward) and 5′-CTAAGAAAACGTGAGGTTGGCGGTC-3′ (reverse); VEGF, 5′-CGAAACCATGAACTTTCTGC-3′ (forward) and 5′-CCTCAGTGGGCACACACTCC-3′ (reverse). Total RNA was normalized using 18S internal standards at a 1:3 ratio (Ambion).

Quantitative real-time PCR was carried out in triplicate with a 10- to 20-fold dilution of first-strand cDNA using human Taqman probes and primers purchased as Assays-on-Demand (Applied Biosystems) for β-glucuronidase (*Gus*, reference gene control) and *VEGF* using an ABI Prism SDS 7000 (Applied Biosystems) according to the manufacturer's instructions. Data were analyzed with ABI Prism SDS 7000 companion software.

VEGF ELISA. For two-dimensional cultures, T4-2 and S1 cells were plated at a density of 500,000 per well, and for three-dimensional cultures, cells were plated at 100,000 per well on top of 200 μL of polymerized lrECM and overlaid with 10% lrECM. Forty-eight hours later, medium was changed to FBM + 0.5% BSA, and 24 h later, secreted VEGF was assayed in triplicate by ELISA (DVE00, R&D Systems) according to the manufacturer's instructions.

Angiogenesis profiling arrays. The relative expression of 84 angiogenesis-related genes was evaluated using the Human Angiogenesis RT^2 Profiler PCR Array system (SuperArray Bioscience Corp.) according to the manufacturer's instructions. DNase-treated total RNA was purified from T4-2 cells treated with either the EGFR-blocking antibody mAb225 or an IgG control. cDNA was generated by reverse transcription from 1 μg of total RNA from each sample using the RT^2 First Strand kit and then combined with the RT^2 qPCR Master Mix and added to lyophilized primer pairs in the 96-well arrays. Thermal cycling was performed in a Bio-Rad iCycler. Relative gene expression levels were calculated using the $\Delta\Delta C_t$ method (27) with normalization to the average expression level of five common genes (*ACTB, B2M, GAPDH, HPRT*, and *RPL13A*).

Microarray analysis. Gene expression analysis was performed on samples of RNA purified from S1 and T4-2 cells grown in three-dimensional lrECM cultures in the presence of various signaling inhibitors or vehicle controls. The Affymetrix High Throughput Array GeneChip system, with HG-U133A chips mounted on pegs in a 96-well format, was used for the analysis, as described (28). Data were imported into the Partek Genomics Suite (Partek, Inc.) and normalized using RMA (29).

Immunoblot analysis. Cells were cultured in three-dimensional lrECM for 72 h, released, and lysed in 10 mmol/L Tris-HCl (pH 7.4), 1 mol/L sodium chloride, 1% Triton X-100, 50 mmol/L sodium fluoride, 1 mmol/L sodium orthovanadate, and protease inhibitor cocktail. Total protein was determined using the bicinchoninic acid assay (Pierce) and 40 μg were electrophoresed on SDS-PAGE, transferred to polyvinylidene difluoride membranes, and blocked with 5% milk. HoxD10 (E-20) polyclonal antibody (Santa Cruz Biotechnology, Inc.), a polyclonal phospho-Akt antibody Ser^{473} (193H12, Cell Signaling), and a mouse monoclonal HIF1α antibody (NB 100-105, Novus Biologicals) were used and detected with enhanced chemiluminescence system (Amersham Biosciences). Relative protein loading was assessed by β-actin (Ab8227, Abcam). Nuclear extracts were isolated from T4-2 and HoxD10-reverted T4-2 cells, and electrophoretic mobility shift assays (EMSA) were performed using procedures as described (30).

Immunofluorescence. After release from three-dimensional lrECM, cells were smeared onto slides and fixed in cold 1:1 methanol-acetone as previously described (23). After blocking with 10% goat serum, cells were incubated overnight with a 1:100 dilution of antibodies against β4 integrin (mAb1964, Chemicon) and washed with immunofluorescence buffer followed by a 1:400 dilution of goat anti-mouse Alexa Fluor 546 IgG (H+L) (Invitrogen), and nuclei were counterstained with 1:1,000 dilution of 4′,6-diamidino-2-phenylindole (DAPI; Sigma). Slides were mounted in Fluoromount G (Southern Biotechnology Associates, Inc.) and images were collected with a Nikon Eclipse TE300 fluorescence microscope.

Ki-67 proliferation index. Proliferation was assessed by Ki-67 immunostaining using a modification of the previous method (23) with a 1:500 dilution of Ki-67 antibody (VP-K451, Vector Laboratories) overnight at 4°C followed by a 1:400 dilution of goat anti-rabbit Alexa Fluor 546 IgG (H+L), counterstained with DAPI, and mounted in Fluoromount G. Proliferation was determined by visually counting at least 300 DAPI-labeled nuclei and thereafter scoring Ki-67–positive cells as a percentage of a total cell number.

Results

Phenotypic reversion of malignant cells restores basal expression of angiogenic factors. Malignant breast epithelial cells (T4-2) cultured in three-dimensional lrECM exhibit a disorganized morphology compared with their growth-arrested, polarized nonmalignant counterparts (S1). Disrupting either β1 integrin, EGFR, MAPK, or PI3K-mediated signaling restores basolateral polarity and growth arrest and reverts malignant cells to a phenotype similar to nonmalignant cells and fails to form tumors *in vivo* (18, 19, 31, 32). We used microarray analysis to determine whether malignant T4-2 cells display enhanced expression of angiogenic factors and whether phenotypic reversion reduces expression of angiogenic factors. We analyzed RNA samples from S1, T4-2, and T4-2 cells reverted with an EGFR inhibitor (AG1478; in duplicate) and T4-2 cells reverted with an EGFR-blocking antibody (mAb225), a β1-integrin–blocking antibody (AIIB2), or inhibitors of MAPK/extracellular signal-regulated kinase (PD98059) and TACE (TAPI-2). Unsupervised hierarchical clustering of all samples (Fig. 1*A*) revealed significantly different transcriptional profiles of S1, T4-2, and reverted T4-2 cells. To identify gene expression changes associated with polarity, we selected genes differentially expressed between disorganized T4-2 colonies, organized nonmalignant S1 colonies, and reverted T4-2 cells ($P < 0.001$, *t* test; Fig. 1*B*). Differentially expressed genes that were significantly higher in T4-2 compared with nonmalignant or reverted T4-2 included several of the Gene Ontology angiogenesis class (GO:0001525; Fig. 1*C*).

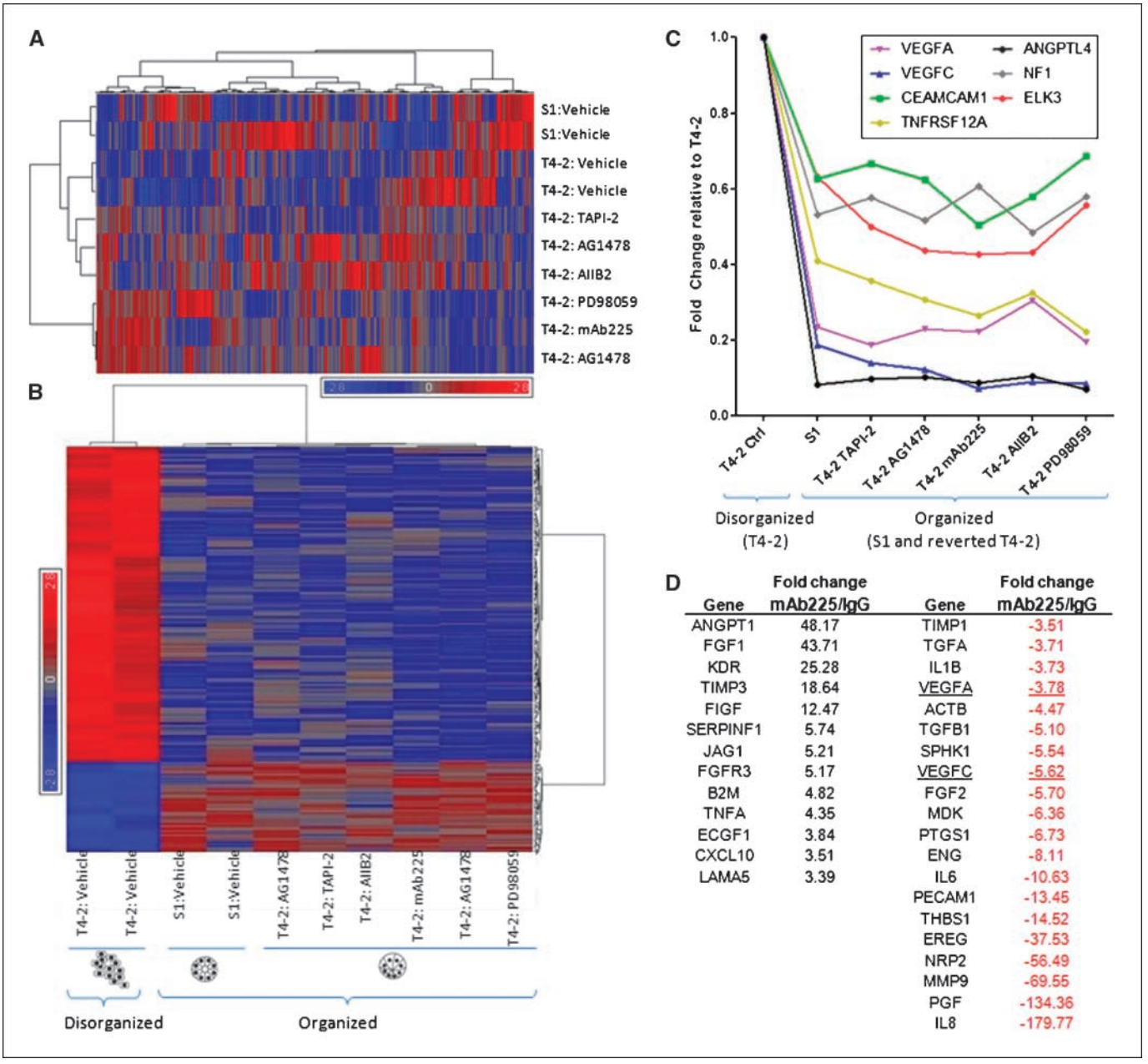

D

Gene	Fold change mAb225/IgG	Gene	Fold change mAb225/IgG
ANGPT1	48.17	TIMP1	-3.51
FGF1	43.71	TGFA	-3.71
KDR	25.28	IL1B	-3.73
TIMP3	18.64	VEGFA	-3.78
FIGF	12.47	ACTB	-4.47
SERPINF1	5.74	TGFB1	-5.10
JAG1	5.21	SPHK1	-5.54
FGFR3	5.17	VEGFC	-5.62
B2M	4.82	FGF2	-5.70
TNFA	4.35	MDK	-6.36
ECGF1	3.84	PTGS1	-6.73
CXCL10	3.51	ENG	-8.11
LAMA5	3.39	IL6	-10.63
		PECAM1	-13.45
		THBS1	-14.52
		EREG	-37.53
		NRP2	-56.49
		MMP9	-69.55
		PGF	-134.36
		IL8	-179.77

Figure 1. Reversion of the malignant phenotype suppresses angiogenic genes. *A,* unsupervised hierarchical clustering using 22,946 probes for 10 variations showing distinct transcriptional profiles of S1, T4-2, and T4-2 cells treated with different drugs. *B,* identification of 294 genes significantly associated ($P < 0.001$) with colony organization in S1, T4-2, and T4-2 cells reverted with different agents. Two hundred four were highly expressed in disorganized (T4-2) colonies and 90 were more highly expressed in organized (S1 and T4-2 reverted) colonies. *C,* profile of seven genes from *B* belonging to the GO:0001525 class of angiogenic regulators high in malignant T4-2 and low in polarized S1 and reverted T4-2 cells. The indicated genes correspond to the following Affymetrix probes: *VEGF*, 210512_at; *VEGFC*, 209946_at; *CEACAM1*, 209498_at; *TNFRSF12A*, 218368_s_at; *ANGPTL4*, 221009_s_at; *NF1*, 211094_s_at; and *ELK3*, 206127_at. *D,* relative fold changes detected in angiogenesis-related genes between control (IgG) or EGFR-blocking antibody (mAb225)–treated T4-2 cells.

For independent confirmation, we performed an RT^2 Profiler PCR array for 84 different angiogenic mediators with RNA isolated from control (IgG) T4-2 and T4-2 reverted with a function-blocking antibody against EGFR (mAb225; Fig. 1*D*). Expression of VEGF and other angiogenic factors, including fibroblast growth factor-2, matrix metalloproteinase-9 (MMP-9), placental growth factor, and VEGF-C (33), was significantly reduced in reverted cells. Thus, expression of angiogenic genes may be restrained when cells adopt a polarized tissue morphology.

Increased VEGF production by breast tumor cells enhances EC migration. To assess a functional role for angiogenic factors linked to tissue polarity, we focused on VEGF. As most soluble inhibitors that revert tumor cells also inhibit signaling in adjacent ECs, we transfected T4-2 cells with HoxD10, which attenuates growth and restores polarity in metastatic breast tumor MDA-MB-231 cells (23). Although T4-2 cells express low levels of HoxD10 mRNA and protein (Fig. 2*A*), restoring expression of HoxD10 did not induce any observable differences in morphology when grown on conventional polystyrene tissue culture plates (Fig. 2*B, top*).

However, when cultured within a three-dimensional lrECM, HoxD10-expressing T4-2 cells formed organized, growth-arrested structures resembling their nonmalignant counterparts, as shown by phase microscopy and immunofluorescent imaging of β4 integrin in which total levels were reduced (data not shown) and the remaining redistributed to the basal surface (Fig. 2*B, bottom*). In three-dimensional lrECM, both nonmalignant S1 and HoxD10-reverted T4-2 cells produced significantly less VEGF compared with control T4-2 cells (Fig. 2*C*). In contrast, when cultured on polystyrene, VEGF mRNA and protein were similar in S1, T4-2, and HoxD10-expressing T4-2 cells (data not shown).

We developed a modified Boyden invasion assay (Fig. 2*D, inset*) to quantify EC migration in response to malignant or nonmalignant cells cultured in lrECM and observed that ECs migrated significantly more in response to coculture with T4-2 cells than S1 cells (Fig. 2*D*). Pretreatment of ECs with VEGF-blocking antibodies reduced EC migration to the basal levels seen in cocultures with S1 cells (Fig. 2*D*), implicating VEGF as the primary mediator of EC migration in EC/T4-2 cocultures. Notably, migration of ECs cocultured with reverted HoxD10-expressing T4-2 cells was significantly reduced to levels observed by blocking VEGF or coculturing with nonmalignant cells (Fig. 2*D*). No differences in EC migration were observed when cocultured with S1, T4-2, or HoxD10-expressing T4-2 cells grown in tissue culture plastic (data not shown).

Together, these data suggest that differential expression of VEGF by nonmalignant and tumorigenic epithelial cells is influenced by their respective tissue architecture.

Phenotypic reversion of metastatic breast tumor cells also suppresses VEGF expression and EC migration. We also compared expression of VEGF in MDA-MB-231 cells, HoxD10-expressing MDA-MB-231 cells, and MDA-MB-231 expressing the paralogous HoxA10 (Fig. 3*A, top*). In contrast to HoxD10, restoring HoxA10 did not induce organized structures in MDA-MB-231 cells in three-dimensional lrECM, as evidenced by diffuse immunofluorescence staining of β4 integrin (Fig. 3*A, bottom*), and growth was

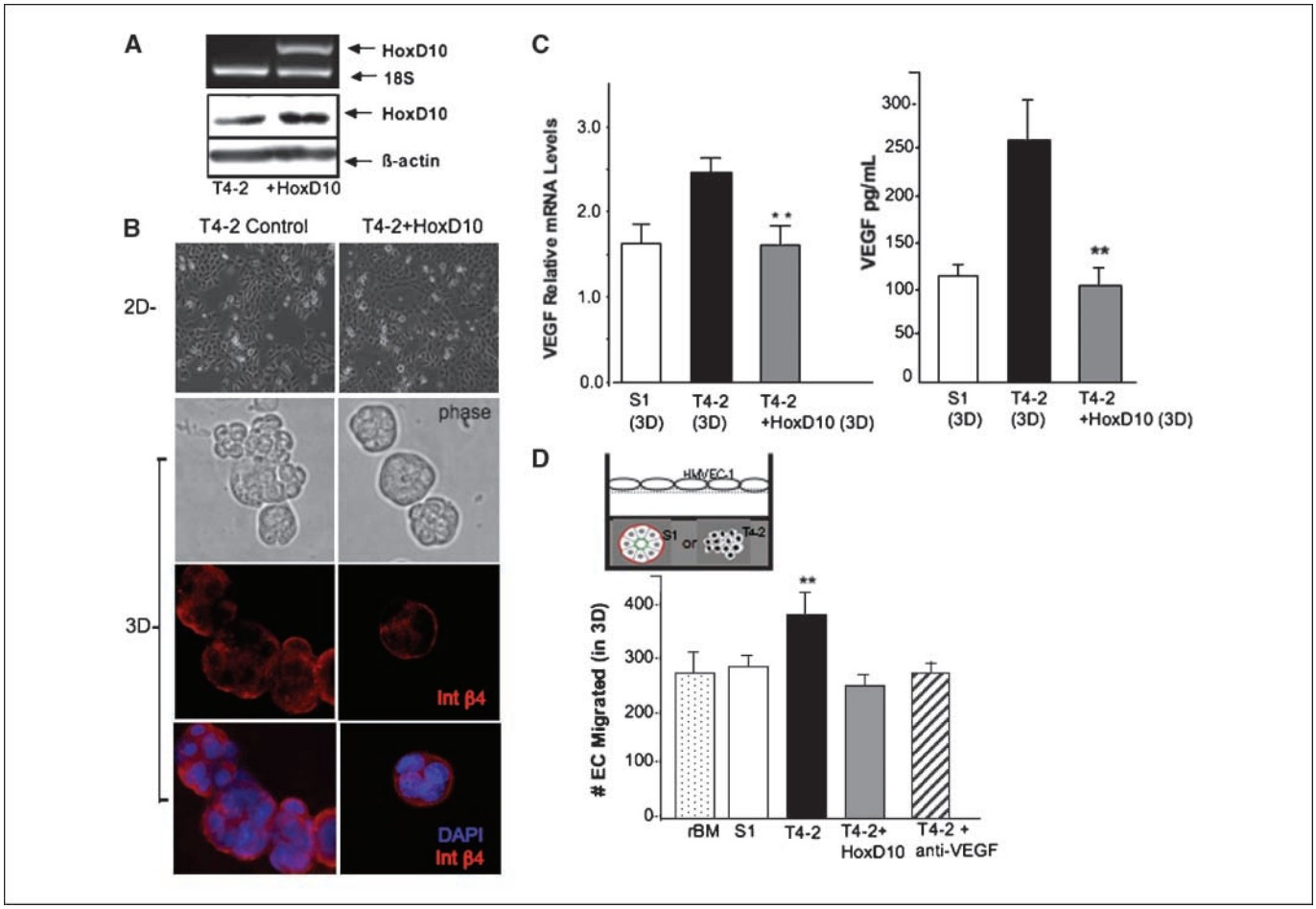

Figure 2. Phenotypic reversion by HoxD10 reduces VEGF and EC migration in three-dimensional cultures. *A, top,* semiquantitative PCR of HoxD10 mRNA in control or HoxD10-transfected T4-2 cells; *bottom,* corresponding Western blot of HoxD10 protein. *B, top,* phase-contrast photomicrographs of control and HoxD10-expressing T4-2 cells on tissue culture plastic for 48 h; *bottom,* phase-contrast photomicrographs, immunofluorescence costaining for β4 integrin (*red*), and merged image with DAPI (*blue*) in control T4-2 or HoxD10-expressing T4-2 cells grown in three-dimensional (*3D*) lrECM for 72 h. *C,* real-time PCR of VEGF mRNA levels in nonmalignant S1 cells, control, or HoxD10-expressing T4-2 cells grown in three-dimensional lrECM for 72 h. **, $P < 0.05$ ($n = 4$). Corresponding ELISA showing relative levels of VEGF protein secreted by S1, T4-2, and HoxD10-reverted T4-2 cells cultured on three-dimensional lrECM for 72 h. **, $P < 0.05$ ($n = 5$). *D, inset,* schematic of coculture model of HMEC-1 on collagen-coated Transwells with either S1, T4-2, or HoxD10-expressing T4-2 cells cultured in three-dimensional lrECM in the lower chambers. Plot shows migration of EC after 4 h of coculture with lrECM only (negative control; *dots*), S1 cells (*white*), T4-2 cells (*black*), HoxD10-expressing T4-2 cells (*gray*), or pretreatment with neutralizing antibody against VEGF (*striped*). *Columns,* mean number of cells that migrated from five different fields (×20) for each of four independent experiments; *bars,* SD. **, $P < 0.05$.

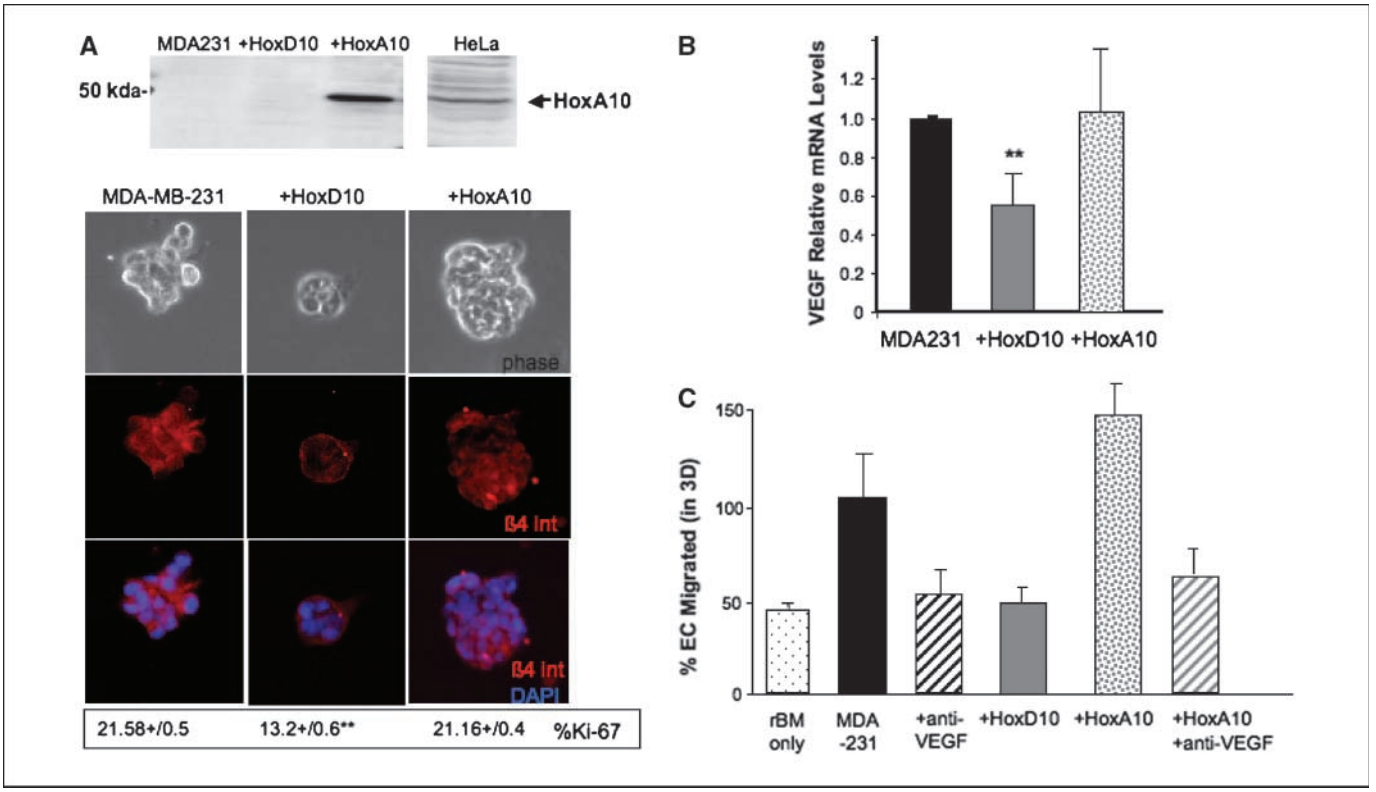

Figure 3. HoxD10, but not HoxA10, down-regulates VEGF and EC migration in metastatic MDA-MB-231 cells. *A, top,* Western blot of HoxA10 in control, HoxD10, or HoxA10-expressing MDA-MB-231 cells and HeLa cells. Corresponding phase-contrast photomicrographs of control, HoxA10, or HoxD10-expressing MDA-MB-231 cells in three-dimensional lrECM for 72 h and immunofluorescence staining for β4 integrin. Proliferation is indicated by the % Ki-67 index expressed as the mean ± SE. **, $P < 0.05$. *B,* real-time PCR of VEGF mRNA in control (*black*), HoxD10-expressing (*gray*), and HoxA10-expressing (*speckled*) MDA-MB-231 cells cultured in three-dimensional lrECM for 72 h. **, $P < 0.05$ ($n = 4$). *C,* migration of EC after 4 h of coculture with lrECM only (negative control; *dots*), control MDA-MB-231 (*black*), and HoxD10-expressing (*gray*) and HoxA10-expressing MDA-MB-231 cells (*speckled*) or EC pretreated with a neutralizing antibody against VEGF and cocultured with control (*dark gray stripes*) or HoxA10-expressing MDA-MB-231 cells (*light gray stripes*), all cultured in three-dimensional lrECM. *Columns,* mean of migrated EC in a total of five different fields (×20) for each of three independent experiments; *bars,* SD. **, $P < 0.05$.

not significantly reduced as determined by Ki-67 labeling (Fig. 3*A*). Importantly, levels of VEGF mRNA remained high in nonpolarized control or HoxA10-expressing cells compared with polarized HoxD10-expressing cells (Fig. 3*B*). EC migration during coculture with MDA-MB-231 could be blocked by antibodies against VEGF or by reexpression of HoxD10 but not by HoxA10 expression (Fig. 3*C*). Thus, only HoxD10, which reverts MDA-MB-231 to a growth-arrested and basally polarized phenotype, attenuates VEGF expression and EC migration.

Sustained growth is not responsible for induction of angiogenic activity. To evaluate whether growth arrest or reestablishment of basolateral polarity was suppressing VEGF, we compared nonmalignant S1 cells with S1 cells constitutively expressing the EGFR (S1-EGFR) that maintained basal polarity in lrECM despite a 10-fold increase in proliferation (19). VEGF expression by proliferating, polarized S1-EGFR cells was not significantly different from growth-arrested S1 cells (Fig. 4*A*). Moreover, there were no significant differences in EC migration in response to S1 or S1-EGFR cells (Fig. 4*B*), indicating that growth arrest was not sufficient to suppress VEGF expression or EC activation.

Reduced VEGF is not linked to reduced HIF1α expression or activity. VEGF can be induced by HIF1α, a transcription factor stabilized by hypoxic tumor microenvironments (34, 35). We investigated whether reduced VEGF expression in reverted tumor cells was accompanied by reduced HIF1α. Western blot analysis shows that relative levels of HIF1α were unchanged in three-dimensional cultures of control T4-2 or reverted T4-2 cells (Fig. 4*C*). We also assessed HIF1α binding to consensus sites in target DNA using EMSA and observed similar levels of bound HIF1α in both control and reverted T4-2 cells (Fig. 4*C*). Thus, reduced VEGF in reverted, polarized tumor cells is not linked to changes in HIF1α expression or activity.

Disruption of polarity is sufficient to increase VEGF expression and EC migration. Given that neither changes in HIF1α nor continued growth in polarized cells induced VEGF expression, we exploited our previous findings that proliferation and polarity are mediated by distinct signaling pathways (22) to establish whether polarity alone regulated VEGF. A dominant-active Rac mutant (Rac1L61) was introduced into HoxD10-expressing T4-2 cells (Fig. 5*A*), which disrupted acinar polarity, as indicated by diffuse β4 integrin staining, without significantly affecting proliferation (Fig. 5*B*). The loss of polarity was accompanied by increased production of VEGF to levels found in nonpolarized control T4-2 cells (Fig. 5*C*) and significantly increased EC migration compared with polarized T4-2 cells expressing only HoxD10-expressing cells (Fig. 5*D*).

Together, these data emphasize that maintaining tissue structure is critical for suppressing VEGF expression and subsequent activation of adjacent EC by malignant cells in the breast tumor microenvironment (Fig. 6).

Discussion

In the present study, we show that production of angiogenic factors and EC activation is primarily controlled by breast epithelial cell polarity and tissue architecture. In conventional (two-dimensional) tissue culture, nonmalignant and malignant breast epithelial cells do not differentially secrete VEGF or recruit ECs. However, once provided with three-dimensional lrECM, nonmalignant cells organize into quiescent, polarized acini, produce low levels of VEGF, and limit migration of cocultured ECs. Disorganized, malignant epithelial cells, on the other hand, produce more VEGF and significantly increase recruitment of ECs, mimicking the stromal angiogenic response of malignant breast tumors *in vivo*. Significantly, phenotypically reverting malignant epithelial cells to polarized acini via reintroduction of the HoxD10 tumor suppressor or by treatment with various signaling inhibitors (20) reduces VEGF and migration of cocultured ECs to levels observed with nonmalignant cells. Hence, differential expression of VEGF by nonmalignant and malignant breast epithelial cells is evident only when cells undergo characteristic morphologic changes in three-dimensional lrECM. Moreover, reduced VEGF transcription in tumor cells repolarized by HoxD10 is unlikely a direct effect, as HoxD10 did not influence VEGF production when cells were unable to reorganize into polarized structures in two-dimensional cultures, although it remains possible that accompanying morphologic changes in three-dimensional cultures unmask binding sites within the VEGF promoter. Still, these findings indicate that activation of the angiogenic switch is not simply due to genetic changes within the tumor cells but rather linked to how cells sense their architecture and interact with their microenvironment.

Importantly, we also show that in tumor cells, which characteristically exhibit increased growth and metabolic demand compared with nonmalignant cells, restoring normal tissue architecture is essential for attenuating their angiogenic potential. Indeed, a 10-fold increase in proliferation of nonmalignant cells was not sufficient to explain resistance to chemotherapeutic agents (17) and is also not sufficient to activate VEGF expression when growing cells maintain a polarized architecture.

Many studies have established that increased proliferation, metabolic demand, and hypoxia in tumor cells stabilize HIF1α

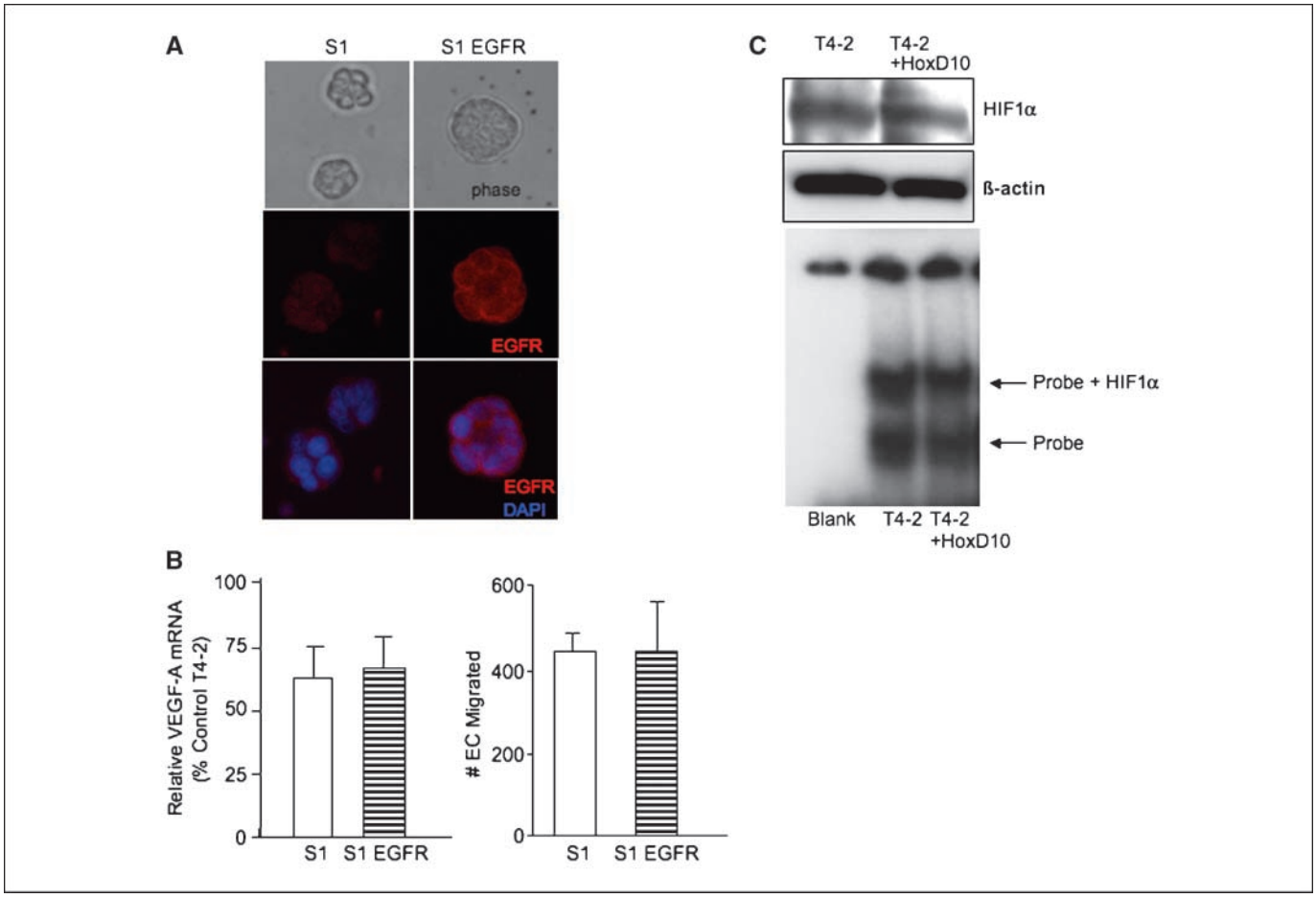

Figure 4. Forced proliferation of polarized breast epithelial cells does not induce VEGF expression or EC migration. *A, top,* phase-contrast photomicrographs of polarized S1 or S1-EGFR cells cultured in three-dimensional lrECM for 72 h; *bottom,* corresponding immunofluorescence staining for EGFR (*red*) and merged image with DAPI staining (*blue*). *B, left,* real-time PCR VEGF mRNA levels in S1 (*white*) or S1-EGFR cells (*horizontal stripes*) cultured in three-dimensional lrECM for 72 h, expressed as percentage of VEGF mRNA levels by malignant T4-2 cells in the same conditions ($n = 4$). *Right,* corresponding EC migration over 4-h coculture with either S1 (*white*) or S1-EGFR cells (*horizontal stripes*) in three-dimensional lrECM in the lower chamber. *Columns,* mean of migrated EC from five different fields (×20) for each of three independent experiments ($n = 4$). *C, top,* Western blot of HIF1α in control T4-2 or HoxD10-expressing T4-2 cells cultured in three-dimensional lrECM for 72 h. Total protein loading is shown by corresponding levels of β-actin. *Bottom,* EMSA with nuclear extracts from control or HoxD10-expressing T4-2 cells incubated with a HIF1α consensus oligonucleotide. *Top arrow,* position of the protein complexes; *bottom arrow,* free, unbound probe.

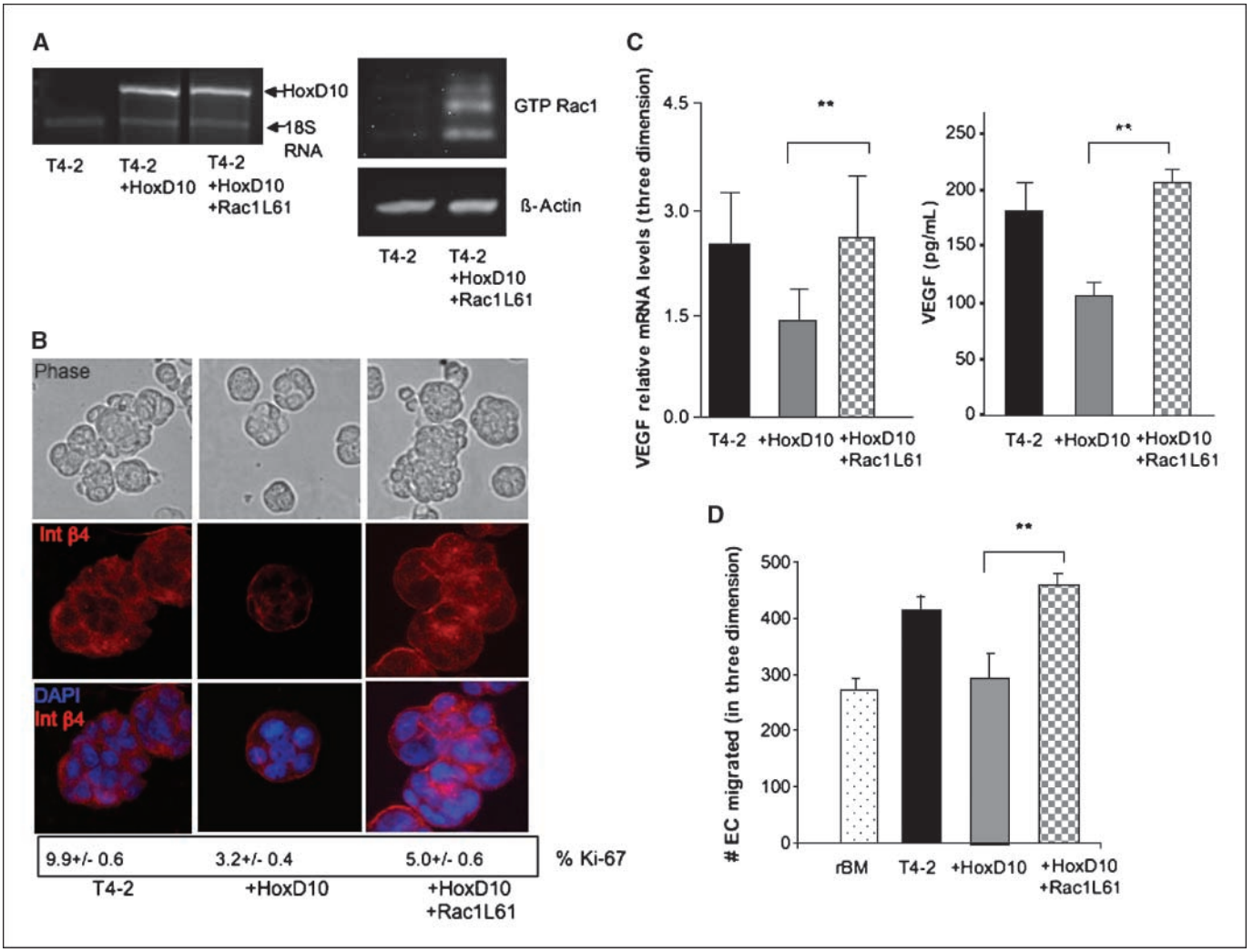

Figure 5. Rac1-mediated disruption of polarity restores VEGF expression and EC migration. *A, left,* levels of HoxD10 in control, HoxD10-expressing, or T4-2 cells expressing both HoxD10 and dominant-active Rac1; *right,* Western blot for GTP-loaded Rac 1 (*top*) in corresponding cells. *Bottom right,* total protein determined by reprobing with β-actin. *B, top,* phase-contrast microscopy of T4-2, HoxD10-expressing T4-2, or T4-2 cells expressing both HoxD10 and Rac1L61 cultured in three-dimensional lrECM for 72 h; *middle,* corresponding immunofluorescence staining for β4 integrin (*red*); *bottom,* merged images for β4 integrin (*red*) and nuclear DAPI (*blue*). Ki-67 labeling index was assessed after 72 h in three-dimensional lrECM; *columns,* mean for 10 independent measurements; *bars,* SE. *C,* real-time PCR showing VEGF mRNA in control T4-2 (*black*), T4-2 cells expressing HoxD10 (*gray*), and T4-2 cells expressing HoxD10 and Rac1L61 (*checkered*) after 72 h in three-dimensional lrECM. **, $P < 0.05$ ($n = 4$). Corresponding ELISA showing VEGF protein secreted by each cell type. **, $P < 0.05$ ($n = 3$). *D,* relative migration of EC over 4 h of coculture with lrECM only (negative control; *dots*), control T4-2 cells (*black*), HoxD10-expressing T4-2 cells (*gray*), and T4-2 cells expressing HoxD10 and Rac1L61 (*checkered*), cultured for 72 h in three-dimensional lrECM. *Columns,* mean of five different fields (×20) for each of three independent experiments. **, $P < 0.05$.

and drive VEGF expression (3, 6, 34–36). Blocking HIF1α expression/activity reduces VEGF expression, and HIF1α-null mice display defective angiogenesis and fail to support tumor growth (8, 35). However, our results show that neither differences in HIF1α expression nor activity underlies reduced VEGF in reverted, polarized tumor cells and implicate other pathways and/or transcriptional mediators in regulating the angiogenic switch in this system.

In a mouse model of pancreatic cancer, hypoxia-independent activation of the angiogenic switch occurs via increased MMP-9 activity, which liberates bioactive VEGF trapped within the tumor matrix (37). Despite the fact that MMP-9 is highly expressed in disorganized T4-2 cells and reduced in reverted T4-2,[4] elevated secretion of VEGF is reflected by increased VEGF mRNA. Whether reduced VEGF transcription by repolarized breast tumor cells increases inhibitory factors (38) and/or attenuates other positive inducers of VEGF requires further investigation.

Previous studies also showed that PI3K signaling induces VEGF (13, 39), and our current study suggests that the Rac1 branch of this pathway directly drives VEGF expression. We reported that PI3K inhibition phenotypically reverts tumorigenic breast epithelial cells and is accompanied by down-regulation of both the Akt and Rac1 effector pathways (22). However, although attenuation of Akt reduces proliferation, it did not restore a polarized phenotype. Instead, suppression of Rac1 activity was necessary for reestablishing an organized polarized phenotype, and selective reactivation of Rac1 disrupts polarity without reinitiating growth when Akt remained blocked (22). Moreover, whereas activation of Rac1 in

[4] A. Beliveau and M.J. Bissell, submitted for publication.

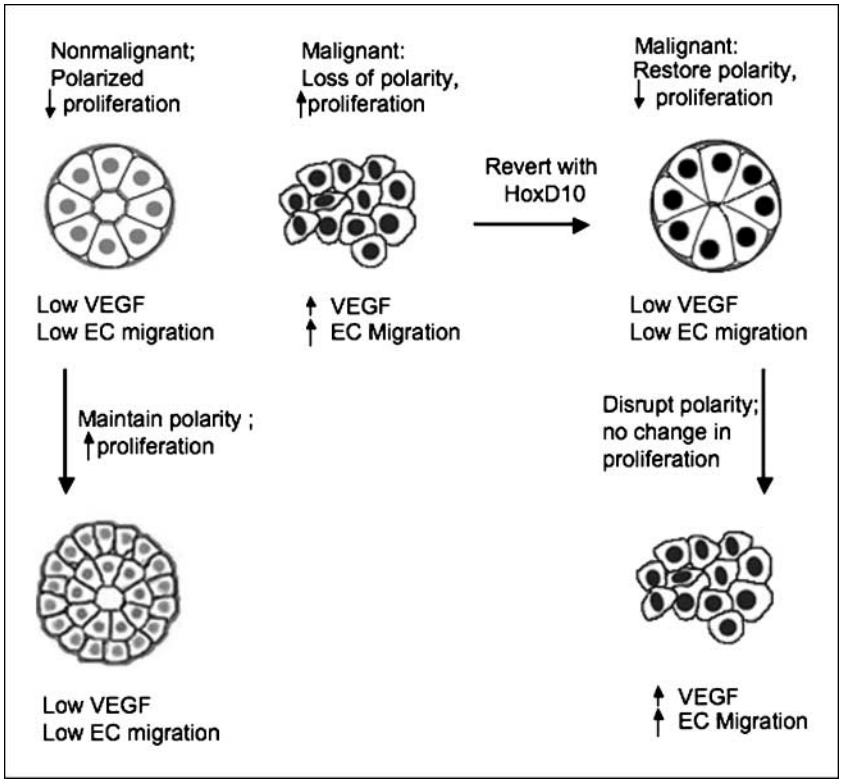

Figure 6. Polarity of breast epithelial cells suppresses VEGF and EC migration. Schematic summarizing the effect of tissue organization on VEGF expression in nonmalignant, malignant, or malignant breast epithelial cells repolarized with HoxD10.

nonmalignant breast epithelial cells normally induces apoptosis, in breast tumor epithelial cells lacking scribble, Rac activation promotes tumorigenesis and loss of cell polarity (40). In the present study, we show that reactivation of Rac1 and disruption of polarity restore VEGF expression and induce EC migration despite the fact that growth remains suppressed via low phospho-Akt levels (latter data not shown).

Active Rac1 directly binds and phosphorylates signal transducer and activator of transcription 3 (STAT3; ref. 41), which in turn forms SP1/STAT3 complexes that bind the VEGF promoter (42) and the SP1 site within the −86 to −66 region of the VEGF promoter is linked to HIF1α-independent transcription of VEGF (10, 39, 43). Phosphorylated STAT3 can also bind to HIF1α and prevent its degradation (44). Although we observed an increase in phospho-STAT3 in Rac1-overexpressing cells, reversion of malignant cells by HoxD10 did not reduce phospho-STAT3 (data not shown) and HIF1α protein levels were similar in both tumorigenic and HoxD10-reverted tumor cells. Thus, binding of STAT3 to either SP1 or HIF and VEGF expression may be context dependent as previously suggested by investigations of pathways impinging on VEGF expression (39), and our current study also emphasizes the critical role of tissue polarity in mediating VEGF expression in breast tumor cells.

It is noteworthy that inhibiting EGFRs represses VEGF in both HIF-dependent and HIF-independent manner, with the latter attributed to reduced phosphorylation and binding of SP1 to the VEGF promoter (43). Several EGFR inhibitors, including those used in this study, not only reduce VEGF expression and inhibit breast tumor angiogenesis *in vivo* but also phenotypically revert tumor cells to a polarized morphology in culture (19, 43, 45, 46). Finally, mice lacking LKB1, a tumor suppressor that directs cell polarity and, when mutated, produces epithelial cancers, show markedly increased VEGF (47, 48).

The present study addresses breast tumor epithelial organization and VEGF production, but it is important to note that other components of the tumor microenvironment, including fibroblasts and macrophages, are also rich sources of angiogenic factors. In DCIS where newly formed capillaries seem immediately adjacent to the basal surface of the breast epithelium (5), the basement membrane is largely intact but most epithelial cells have lost their characteristic polarized morphology and display attenuated expression of the HoxD10 tumor suppressor (3, 23). As macrophage recruitment typically occurs in later stages of malignant progression accompanied by basement membrane degradation (49), it is likely that the loss of epithelial cell polarity marks an early and critical step in activation of the angiogenic switch.

Disclosure of Potential Conflicts of Interest

No potential conflicts of interest were disclosed.

Acknowledgments

Received 10/23/08; revised 5/7/09; accepted 5/26/09; published OnlineFirst 8/4/09.

Grant support: California Breast Cancer Research Program Award 101B-0157 (N. Boudreau); U.S. Department of Energy, OBER Office of Biological and Environmental Research (DE-AC02-05CH1123), a Distinguished Fellow Award, and Low Dose Radiation Program and the Office of Health and Environmental Research, Health Effects Division (03-76SF00098; M. Bissell); National Cancer Institute awards R01CA064786, R01CA057621, U54CA126552, and U54CA112970; and U.S. Department of Defense grants W81XWH0810736 and W81XWH0510338.

The costs of publication of this article were defrayed in part by the payment of page charges. This article must therefore be hereby marked *advertisement* in accordance with 18 U.S.C. Section 1734 solely to indicate this fact.

References

1. Folkman J. Tumor angiogenesis. Adv Cancer Res 1974;19:331–58.
2. Folkman J, Hahnfeldt P, Hlatky L. Cancer: looking outside the genome. Nat Rev Mol Cell Biol 2000;1:76–9.
3. Brown LF, Guidi AJ, Schnitt SJ, et al. Vascular stroma formation in carcinoma *in situ*, invasive carcinoma, and metastatic carcinoma of the breast. Clin Cancer Res 1999;5:1041–56.
4. Engels K, Fox SB, Harris AL. Angiogenesis as a biologic and prognostic indicator in human breast carcinoma. EXS 1997;79:113–56.
5. Engels K, Fox SB, Whitehouse RM, Gatter KC, Harris AL. Distinct angiogenic patterns are associated with high-grade *in situ* ductal carcinomas of the breast. J Pathol 1997;181:207–12.
6. Knowles HJ, Harris AL. Hypoxia and oxidative stress in breast cancer. Hypoxia and tumourigenesis. Breast Cancer Res 2001;3:318–22.
7. Shojaei F, Ferrara N. Antiangiogenic therapy for cancer: an update. Cancer J 2007;13:345–8.
8. Giordano FJ, Johnson RS. Angiogenesis: the role of the microenvironment in flipping the switch. Curr Opin Genet Dev 2001;11:35–40.
9. Boudreau N, Myers C. Breast cancer-induced angiogenesis: multiple mechanisms and the role of the microenvironment. Breast Cancer Res 2003;5:140–6.
10. Arsham AM, Howell JJ, Simon MC. A novel hypoxia-inducible factor-independent hypoxic response regulating mammalian target of rapamycin and its targets. J Biol Chem 2003;278:29655–60.
11. Proud G. Regulation of mammalian translation factors by nutrients. Eur J Biochem 2002;269:5338–49.
12. Chung J, Bachelder RE, Lipscomb EA, Shaw LM, Mercurio AM. Integrin ($\alpha6\beta4$) regulation of eIF-4E activity and VEGF translation: a survival mechanism for carcinoma cells. J Cell Biol 2002;158:165–74.
13. Price DJ, Avraham S, Feuerstein J, Fu Y, Avraham HK. The invasive phenotype in HMT-3522 cells requires increased EGF receptor signaling through both PI 3-kinase and ERK 1,2 pathways. Cell Commun Adhes 2002;9:87–102.
14. Reddy KB, Krueger JS, Kondapaka SB, Diglio CA. Mitogen-activated protein kinase (MAPK) regulates the expression of progelatinase B (MMP-9) in breast epithelial cells. Int J Cancer 1999;82:268–73.
15. Easwaran V, Lee SH, Inge L, et al. β-Catenin regulates vascular endothelial growth factor expression in colon cancer. Cancer Res 2003;63:3145–53.
16. Care A, Felicetti F, Meccia E, et al. HOXB7: a key factor for tumor-associated angiogenic switch. Cancer Res 2001;61:6532–9.
17. Weaver VM, Lelievre S, Lakins JN, et al. $\beta4$ Integrin-dependent formation of polarized three-dimensional architecture confers resistance to apoptosis in normal and malignant mammary epithelium. Cancer Cell 2002;2:205–16.
18. Weaver VM, Petersen OW, Wang F, et al. Reversion of the malignant phenotype of human breast cells in three-dimensional culture and *in vivo* by integrin blocking antibodies. J Cell Biol 1997;137:231–45.
19. Wang F, Weaver VM, Petersen OW, et al. Reciprocal interactions between $\beta1$-integrin and epidermal growth factor receptor in three-dimensional basement membrane breast cultures: a different perspective in epithelial biology. Proc Natl Acad Sci U S A 1998;95:14821–6.
20. Bissell MJ, Kenny PA, Radisky DC. Microenvironmental regulators of tissue structure and function also regulate tumor induction and progression: the role of extracellular matrix and its degrading enzymes. Cold Spring Harb Symp Quant Biol 2005;70:343–56.
21. Petersen OW, Ronnov-Jessen L, Howlett AR, Bissell MJ. Interaction with basement membrane serves to rapidly distinguish growth and differentiation pattern of normal and malignant human breast epithelial cells. Proc Natl Acad Sci U S A 1992;89:9064–8.
22. Liu H, Radisky DC, Wang F, Bissell MJ. Polarity and proliferation are controlled by distinct signaling pathways downstream of PI3-kinase in breast epithelial tumor cells. J Cell Biol 2004;164:603–12.
23. Carrio M, Arderiu G, Myers C, Boudreau NJ. Homeobox D10 induces phenotypic reversion of breast tumor cells in a three-dimensional culture model. Cancer Res 2005;65:7177–85.
24. Chu MC, Selam FB, Taylor HS. HOXA10 regulates p53 expression and Matrigel invasion in human breast cancer cells. Cancer Biol Ther 2004;3:568–72.
25. Ades EW, Candal FJ, Swerlick RA, et al. HMEC-1: establishment of an immortalized human microvascular endothelial cell line. J Invest Dermatol 1992;99:683–90.
26. Myers C, Charboneau A, Cheung I, Hanks D, Boudreau N. Sustained expression of homeobox D10 inhibits angiogenesis. Am J Pathol 2002;16:2099–109.
27. Pfaffl MW. A new mathematical model for relative quantification in real-time RT-PCR. Nucleic Acids Res 2001;29:e45.
28. Kenny PA, Lee GY, Myers CA, et al. The morphologies of breast cancer cell lines in three-dimensional assays correlate with their profiles of gene expression. Mol Oncol 2007;1:84–96.
29. Irizarry RA, Bolstad BM, Collin F, Cope LM, Hobbs B, Speed TP. Summaries of Affymetrix GeneChip probe level data. Nucleic Acids Res 2003;31:e15.
30. Mace KA, Yu DH, Paydar KZ, Boudreau N, Young DM. Sustained expression of Hif-1α in the diabetic environment promotes angiogenesis and cutaneous wound repair. Wound Repair Regen 2007;15:636–45.
31. Wang F, Hansen RK, Radisky D, et al. Phenotypic reversion or death of cancer cells by altering signaling pathways in three-dimensional contexts. J Natl Cancer Inst 2002;94:1494–503.
32. Kenny PA, Bissell MJ. Targeting TACE-dependent EGFR ligand shedding in breast cancer. J Clin Invest 2007;117:337–45.
33. Adams RH, Alitalo K. Molecular regulation of angiogenesis and lymphangiogenesis. Nat Rev Mol Cell Biol 2007;8:464–78.
34. Brugarolas J, Kaelin WG, Jr. Dysregulation of HIF and VEGF is a unifying feature of the familial hamartoma syndromes. Cancer Cell 2004;6:7–10.
35. Covello KL, Simon MC. HIFs, hypoxia, and vascular development. Curr Top Dev Biol 2004;62:37–54.
36. Bos R, Zhong H, Hanrahan CF, et al. Levels of hypoxia-inducible factor-1α during breast carcinogenesis. J Natl Cancer Inst 2001;93:309–14.
37. Bergers G, Brekken R, McMahon G, et al. Matrix metalloproteinase-9 triggers the angiogenic switch during carcinogenesis. Nat Cell Biol 2000;2:737–44.
38. Harper J, Yan L, Loureiro RM, et al. Repression of vascular endothelial growth factor expression by the zinc finger transcription factor ZNF24. Cancer Res 2007;67:8736–41.
39. Reisinger K, Kaufmann R, Gille J. Increased Sp1 phosphorylation as a mechanism of hepatocyte growth factor (HGF/SF)-induced vascular endothelial growth factor (VEGF/VPF) transcription. J Cell Sci 2003;116:225–38.
40. Zhan L, Rosenberg A, Bergami KC, et al. Deregulation of scribble promotes mammary tumorigenesis and reveals a role for cell polarity in carcinoma. Cell 2008;135:865–78.
41. Simon AR, Vikis HG, Stewart S, Fanburg BL, Cochran BH, Guan KL. Regulation of STAT3 by direct binding to the Rac1 GTPase. Science 2000;290:144–7.
42. Loeffler S, Fayard B, Weis J, Weissenberger J. Interleukin-6 induces transcriptional activation of vascular endothelial growth factor (VEGF) in astrocytes *in vivo* and regulates VEGF promoter activity in glioblastoma cells via direct interaction between STAT3 and Sp1. Int J Cancer 2005;115:202–13.
43. Pore N, Jiang Z, Gupta A, Cerniglia G, Kao GD, Maity A. EGFR tyrosine kinase inhibitors decrease VEGF expression by both hypoxia-inducible factor (HIF)-1-independent and HIF-1-dependent mechanisms. Cancer Res 2006;66:3197–204.
44. Jung JE, Kim HS, Lee CS, et al. STAT3 inhibits the degradation of HIF-1α by pVHL-mediated ubiquitination. Exp Mol Med 2008;40:479–85.
45. Muthuswamy SK, Li D, Lelievre S, Bissell MJ, Brugge JS. ErbB2, but not ErbB1, reinitiates proliferation and induces luminal repopulation in epithelial acini. Nat Cell Biol 2001;3:785–92.
46. Izumi Y, Xu L, di Tomaso E, Fukumura D, Jain RK. Tumour biology: Herceptin acts as an anti-angiogenic cocktail. Nature 2002;416:279–80.
47. Baas AF, Kuipers J, van der Wel NN, et al. Complete polarization of single intestinal epithelial cells upon activation of LKB1 by STRAD. Cell 2004;116:457–66.
48. Ylikorkala A, Rossi DJ, Korsisaari N, et al. Vascular abnormalities and deregulation of VEGF in Lkb1-deficient mice. Science 2001;293:1323–6.
49. Pollard JW. Macrophages define the invasive microenvironment in breast cancer. J Leukoc Biol 2008;84:623–30.